Image quality in coronary CT angiography: challenges and technical solutions

Peer-reviewed author version

GHEKIERE, Olivier; Salgado, Rodrigo; Buls, Nico; Leiner, Tim; Mancini, Isabelle; Vanhoenacker, Piet; DENDALE, Paul & Nchimi, Alain (2017) Image quality in coronary CT angiography: challenges and technical solutions. In: BRITISH JOURNAL OF RADIOLOGY, 90(1072).

DOI: 10.1259/bjr.20160567
Handle: http://hdl.handle.net/1942/24277

Image quality in Coronary CT Angiography: Challenges and technical solutions

Short title:

Image quality in Coronary CT Angiography

Review article

Olivier Ghekiere[1,2,3], MD; Rodrigo Salgado[4], MD; Nico Buls[5], PhD, Tim Leiner[6], MD, PhD; Isabelle Mancini[1], MSc; Piet Vanhoenacker[7], MD, PhD; Paul Dendale[8], MD, PhD; Alain Nchimi[9], MD, PhD

(1) Department of Radiology, Centre Hospitalier Chrétien (CHC)

Rue de Hesbaye, 75

B-4000 Liège, Belgium

(2) Department of Radiology, Jessa Ziekenhuis

Stadsomvaart 11

B- 3500 Hasselt, Belgium

(3) Faculty of Medicine and Life Sciences, Hasselt University

Agoralaan, Building A and C

B-3500 Hasselt, Belgium

(4) Department of Radiology, Antwerp University Hospital (UZA)

Wilrijkstraat 10

B- 2650 Edegem, Belgium

(5) Department of Radiology, UZ Brussel

Laarbeeklaan 103

B- 1090 Brussels, Belgium

(6) Department of Radiology, Utrecht University Medical Center

Heidelberglaan 100

NL-3584 CX Utrecht, The Netherlands

(7) Department of Radiology, OLV ziekenhuis Aalst

Moorselbaan 164

B-9300 Aalst, Belgium

(8) Heart Center Hasselt, Jessa Ziekenhuis

Stadsomvaart, 11

B- 3500 Hasselt, Belgium

(9) GIGA cardiovascular sciences, Liège University (ULg)

Domaine universitaire du Sart Tilman, Rue de l'hôpital, 1

B-4000 Liège, Belgium

Address for correspondence

Olivier Ghekiere, MD

Department of Radiology, Centre Hospitalier Chrétien (CHC)

Rue de Hesbaye, 75

B-4000 Liège, Belgium

Phone: +32-4-2248800

Fax: +32-4-2248810

Department of Radiology, Jessa Ziekenhuis

Stadsomvaart 11

B-3500 Hasselt, Belgium

Phone: +32-11-338000

Fax: +32-11-338008

olivierghekiere@gmail.com

Abstract

Multidetector CT angiography has become a widely accepted examination for non-invasive evaluation of the heart and coronary arteries. Despite its ongoing success and worldwide clinical implementation, it remains an often-challenging procedure in which image quality, and hence diagnostic value, is determined by both technical and patient-related factors. Thorough knowledge of these factors is important to obtain high quality examinations. In this review, we discuss several key elements that may adversely affect coronary CT angiography image quality as well as potential measures that can be taken to mitigate their impact. In addition, several recent vendor-specific advances and future directions to improve image quality are discussed.

Keywords: Coronary CT angiography; technical principles; artifacts; image quality; technological advances.

1. Introduction

The high negative predictive value of coronary CT angiography (CTA) makes it a suitable tool for excluding significant coronary artery disease (CAD).[1] Coronary CTA is technically complex and places a greater emphasis on scanning technologies than any other type of CT examination. Indeed, coronary arteries both have small caliber and varying degrees of motion during the cardiac cycle.[2] Image quality can be degraded by many patient- and technique related factors. Image artifacts are causes for misinterpretation, making the diagnostic accuracy of Coronary CTA to a great extent dependent on their recognition and operator-awareness.[2, 3] Potential problems related to these artifacts include insufficient tissue-contrast, limited spatial and temporal resolution and inadequate volume coverage. The aim of this review is to discuss these technical issues, important recent vendor-specific solutions as well as future directions.

2. Image quality in coronary CTA

The basic principle of Coronary CTA is to acquire a motion-free volumetric dataset through the heart during peak coronary artery enhancement. The final image quality and associated radiation exposure are determined by both technical and patient-related factors. Image quality is therefore a complex entity for which there is no single objective scale. It has been recently established that coronary artery size is an important parameter in determining image quality.[4] While spatial resolution, as discussed in the next paragraph, is the only objective method to evaluate image detail, other factors have been discussed in the literature. In practice, the final endpoint of all factors influencing coronary CTA image quality is their impact on image interpretation, which assumes that all of the following quantitative or qualitative variables scaling should be within an "acceptable" range: noise, vascular enhancement and coronary motion.

Image noise is one of the principal determinants of image quality, and mainly depends on the number of x-ray photons reaching the detector. Image noise is influenced by technical and patient-related parameters (e.g. weight and anatomy), regardless of the filters used during the image reconstruction process to achieve the desired amount of image sharpness versus noise. Image noise can be measured quantitatively by placing a region-of-interest (ROI) in contrast-enhanced structures (e.g. left ventricle cavity or thoracic aorta). The then obtained standard deviation of the HU-values within the ROI area is a measure of image noise. Background noise can also be considered as the standard deviation of a ROI within the air (e.g. trachea or main bronchus).[5] Although no standard cut-off values of image noise have been reported, some authors suggested values of ≤30HU for improved coronary CTA image quality. [6-8]

Besides image noise, image interpretability is further influenced by the degree of *vascular enhancement*. Previous reports have suggested that a vascular attenuation value of more than 400 HU in the aorta is required for coronary CTA image interpretability. [6-10]

While vascular enhancement and image noise both are defining parameters in determining image quality, in practical terms it is more useful to use the *signal-to-noise (SNR) ratio. SNR* is a generic term to indicate how much signal versus how much noise a particular image has. Similarly, *contrast-to-noise ratio (CNR)* is determined by the differences in CT density values between different materials versus the background noise.

When image noise and vascular enhancement are adequate, the remaining interpretability factors are *motion-related*. These are subjective by nature, evaluated visually as apparent blurring of the coronary artery contours and luminal visualization using Likert scales.[4, 11, 12]

3. Factors affecting image quality

Technical parameters mainly include temporal resolution, spatial resolution, contrast resolution and radiation dose. It is further essential to synchronize image acquisition with cardiac motion by

simultaneous ECG recording. These technical factors are closely linked with each other in terms of balancing image quality versus radiation exposure.[3, 13]

Temporal resolution is the minimal time necessary to compile all X-ray data that are required to calculate or reconstruct one cross sectional CT data set. High temporal resolution is required in coronary CTA to ensure motion-free image quality of the fast moving coronary arteries. The most relevant parameter with a proportional impact on temporal resolution is the rotation speed of the gantry tube.

S*patial resolution* defines the ability of a CT scanner to discern high-contrast anatomic details and is often specified in terms of line pairs per centimeter obtained from phantom scans. It must be considered both in the scan x-y plane (in-plane) as well as in the z-direction (through-plane). Technically, the full width half maximum (FWHM) of the point spread function (PSF) expresses the performance of CT scanners with regard to spatial resolution. The FWHM defines whether two adjacent structures will be represented separately in the images; two structures separated by at least one FWHM can in general be distinguished from each other, whereas two structures separated by less than one FWHM are bound to merge together in the reconstructed image. As such, the spatial resolution depends on the detector properties, but also on the reconstruction filter used, the object contrast and image noise. Since this information is not available on images, the voxel size is often used as an alternative surrogate marker.[14]

Voxel size depends on pixel size within the axial image and through-plane resolution. It is determined by the matrix (e.g. 512 x 512) and the field of view (FOV), whereas through-plane resolution depends on the detector aperture width and focal spot size. According to the Nyquist frequency equation, the minimal coronary diameter evaluable without sampling error should be at

least the double of the voxel size.[3] An intrinsic spatial resolution (expressed as FWHM) of about 0.5–0.7 mm, a voxel size of about 0.5 mm x 0.5 mm x 0.5 mm or smaller are, in general, adequate to image most of the coronary arteries.

Fast coverage of the entire heart using the shortest acquisition time helps to avoid breathing-related artifacts, which can be achieved by increasing detector size and therefore anatomic coverage per rotation. In current multidetector CT (MDCT) scanners, detector arrays (N x T) range from about 40 mm to 160 mm, where T is the individual slice thickness and N is the number of simultaneously acquired slices. When the whole heart is within the anatomic detector coverage per rotation, no table movement is necessary. Otherwise, a varying amount of table movements and number of heart cycles is necessary to ensure complete cardiac coverage. The associated pitch is defined as the ratio of table feed (TF) per rotation to the detector coverage; p = TF /(N x T), with typical values in CCTA ranging from 0.2 to 0.4 with single x-ray tube scanners, and up to 3 with a dual-source CT (DSCT).[13]

The often used term "Contrast resolution" refers to the smallest difference in material density that can be detected between adjacent objects, it is often described as percentage (%) density difference at a defined exposure level.

Radiation exposure can be quantitatively assessed by standard technical dose descriptors: the volume CT Dose Index ($CTDI_{vol}$; mGy) and Dose Length Product (DLP; mGycm). The estimated effective dose (E; mSv) represents the biological risk by the whole body dose to a reference human. It is preferably estimated by using a detailed computational organ dose model that accounts for selected techniques, anatomical location of the scan and patient size.[15, 16] For practical reasons, a rough estimate can also be provided by using a general DLP to E conversion coefficient, the so-

called k-factors that are determined by the anatomical location. The reported use of conversion factors that are established for conventional chest CT (k = 0.014-0.017 mSv x (mGy x cm)$^{-1}$ tend to severely underestimate the E in coronary CTA, where a value of k = 0.026 mSv x (mGy x cm)$^{-1}$ is more appropriate.[15] The estimation of E remains problematic for partial body exposure, with an inherent relative uncertainty of approximately ± 40%.[17] Therefore, the exact impact of dose reducing strategies should be evaluated by using technical dose descriptors. Nevertheless, E remains valuable to compare dose between anatomic regions and with other imaging modalities. Radiation dose is closely related with image quality, and both are influenced by virtually all patient-specific and CT acquisition parameters, including tube current (mA), energy (kilovoltage (kV)), gantry rotation speed, scanning length and table speed.[17]

4. Image quality failure and artifacts

Image artifacts usually result from the failure of previously mentioned determinants of image quality. Clinically relevant artifacts on CCTA and their potential solutions are summarized in Table 1. The most common artifacts are related to cardiac, pulmonary or bulk body motion, resulting in coronary artery *blurring* (Figure 1) and *stairstep artifacts* (Figure 2). Their presence depends on the scanner's temporal resolution, but also on the presence of extra-cardiac movement such as respiratory or voluntary motion.

Blurring occurs when the temporal resolution is insufficient to accurately register the moving targeted structure (e.g. when data sampling exceeds the diastolic rest period, either due to a high heart rate (HR), or due to the selection of an inappropriate reconstruction window). The right

coronary artery is most commonly affected due to its higher velocity and range of motion compared with other coronary segments.[2]

Banding or stairstep artifacts are section gaps in imaging data due to cardiac phase misregistrations between consecutive gantry rotations. The most frequent causes are arrhythmia or HR variation during acquisition.

Beam hardening is caused by an increase in mean photon energy of the X-ray beam when it passes through a cross-section with heterogeneous density. The lower energy photons of the polychromatic beam are primarily absorbed, resulting into a higher mean energy of the beam when it reaches the detector. It results in dark bands throughout the image, the so-called *streak artifacts*. In practice, these artifacts are typically generated by highly attenuating structures or interfaces such as high iodine concentration (e.g. in the superior vena cava), surgical clips and metallic implants (pacemaker, stent struts).

In Blooming artifacts, high attenuating objects appear larger than they are. This results from multiple factors, including inadequate photon energy and partial volume effect; the latter caused by insufficient temporal and spatial resolution particularly in the z-direction.[13] Coronary stents, and to some extent vascular calcifications, are of special importance for attenuation-related effects as they generate both *streak- and blooming artifacts*, causing inappropriate vessel lumen visibility or in-stent visualization due to motion, partial volume effect, and beam hardening (Figure 3).

Blooming artifact magnitude and stent lumen visibility largely depend on stent size, strut thickness, material and mesh design.[18] Magnesium stents are far more favourable for Coronary CTA than tantalum-coated stents with up to 90% in-stent visibility, depending on stent size.[19]

Helical artifacts with their typical *windmill-like* appearance are seen in moving objects during spiral acquisition, or in cases with ECG synchronization failure. The table movement during the acquisition results in projections from slightly different parts of the object. In coronary artery segments that are obliquely oriented along the z-axis, this spiral interpolation process results in hypodense areas surrounding the vessels (Figure 4).

Finally, image artifacts can also theoretically be caused by *low-attenuating* objects such as air bubbles introduced in the right heart or pulmonary artery during contrast material administration or in the mediastinum after surgery.[2, 3] In practice, the hypodense zones surrounding these air bubbles do not alter coronary visibility.

5. Image quality improvement strategies

All the major CT scanner vendors have devised their own proprietary solutions for approaching the key artifacts and technical limitations discussed above (Figure 5 and Table 2).

Besides the discussed technical parameters, a successful coronary CTA also depends on proper patient selection and preparation (Figure 6). Furthermore, as with every CT angiography examination, a strong and homogenous arterial enhancement of the coronary arteries is required. Important parameters to consider here include contrast agent volume, iodine concentration, injection speed and bolus duration, which should be adjusted to the body habitus of the patient (e.g. body mass index (BMI)).[20] Intraluminal contrast attenuation, a determinant of image quality, is also influenced by other technical parameters [21], as e.g. it has been showed that lowering the kilovoltage from 120 to 100 kV not only reduces radiation exposure, but results also in a significant increase (27-36%) of the vascular attenuation at the same injection rate. This is due to the higher

attenuation of iodine at lower energy.[22, 23] However, image noise is also increased in the range of 16-81 % [22, 24], which allows further decrease of the tube energy to 80 kV only in children and adults with low BMI.[21, 25] A more extensive discussion falls outside the scope of this review.

Patient selection and preparation

Patients with heavily calcified coronary arteries are subject to a higher rate of false-positive examinations, owing mainly to streak and blooming artifacts generated by these high-density structures.[26, 27] Even with 64-slice and newer CT systems, the sensitivity and specificity of coronary CTA for significant stenosis remains high in the presence of severe calcifications.[28] Because motion further intensifies calcium-related artifacts [26], patients should be screened for compliance to breathhold and HR stability. Depending on the temporal resolution of the scanner, patients with irregular HR or HR above a certain limit (typically 65 beats per minute (bpm)) are pre-medicated with beta-blockers in some facilities, both to improve image quality and reduce radiation exposure. However, efficacy of beta-blocker administration to consequently achieve the targeted HR remains subject of discussion.[29] In patients with relative or absolute contraindications to beta-blocker administration, calcium-channel blockers and ivabradine are known alternatives.[30]

Finally, the administration of 0.4 mg sublingual nitrogycerin prior to coronary CTA increases the coronary diameter for improved image quality, especially for smaller branches.[31]

Hardware solutions

Significant advances have taken place during the last decade for the main scanner hardware component, the *gantry*, containing the tube(s) and detectors. All vendors have placed a critical emphasis on the improvement of the gantry rotation speed and (varying across vendors) the

increase of number of detectors, as such improving the data acquisition. [12, 32] Scan duration should be as short as possible to limit motion artifacts of the fast moving coronary arteries.

In coronary CTA, partial reconstruction algorithms allow image reconstruction from data acquired within a half gantry rotation; the so-called half-scan.[3] This may be confusing, since the X-ray fan beam angle of the CT detectors (approximately 50°) plus a transition angle for smooth data weighting should be added to the 180° rotation, resulting in a minimal rotation of approximately 260° for image reconstruction.[13] The influence of the fan angle increases if the positioning of the heart deviates from the center of the scan field, resulting in lower temporal resolution. The maximal tube rotation speed of current scanners is within the range of 250-350 ms (Table 2). Additional hardware-based improvements of temporal resolution have been made possible with DSCT. DSCT are constructed with two X-ray tubes at an angle of approximately 90°, and two corresponding detector rows within a single gantry, resulting in a two-fold increased temporal resolution in comparison to single source scanners.

Scanner tubes have benefited from flying focal spot technologies, along with improved power and cooling capacities. Emphasis on *detector* properties has led to increased sensitivity to photons, along with reduced collimation and reduced refractory period between detected pulses. Since spatial resolution of MDCT is influenced by collimation and focal spot size[13], it has especially improved since the introduction of submillimeter (0.5-0.625 mm) detector size elements. Recent detector technologies, along with tube energy rapid switching capacity and dual-source in some vendors, have made dual-energy scanning possible which allows assessment of the x-ray absorption spectra from a broad range of monoenergetic exposure. Regarding image quality, dual-energy acquisitions allow the reconstruction of the anatomy at both a (virtual) low and high energy

(keV) [33], which may be helpful to mitigate streak artifacts or assess tissue iodine concentration. Increased detector's coverage to 8- and 16-cm per gantry rotation using 256- and 320-row detector scanners respectively, currently enables heart coverage with minimal or even no table movement. Image acquisition time is shortened, requiring a minimal number of heartbeats (ideally one) and a shorter breath-hold, with less susceptibility to the occurrence of arrhythmias or ectopic beats. An alternative approach for obtaining single heart beat coverage is by using fast table movement (high-pitch) spiral acquisition protocols, currently only possible with DSCT systems.[34]

Software solutions

One of the specific challenges of Coronary CTA is correct ECG *synchronization of the data acquisition to the HR of the patient*. ECG synchronization can be either prospective or retrospective. With retrospective ECG-gated techniques, scanning is performed throughout the entire cardiac cycle. After all data has been obtained, a user-defined reconstruction of the desired segments of the cardiac cycle is performed, corresponding to the optimal phase of the coronary arteries with least coronary motion. Conversely, in prospective ECG-triggering, scanning is only performed during a pre-defined segment of the cardiac cycle; typically at end-diastole in lower and stable heart rates.

Temporal resolution is further influenced by the choice between *mono- and multisegment reconstruction* (Figure 7). The mono-segment reconstruction mode is typically applied in HR < 65-75 bpm, the upper limit depending on the effective temporal resolution (gantry rotation time) of the available equipment. When used in higher HR, the delivered temporal resolution is insufficient to provide high quality images. In such instances, multisegment reconstruction is typically used to improve the temporal resolution. In multisegment acquisitions, several partial scans at a given

position are acquired, multiplying the temporal resolution by a factor equal to the number of segments. Contrary to monosegment reconstructions, at least two heartbeats are needed, which can be acquired prospectively or retrospectively. Multisegment data acquisition can be applied in a prospective triggering mode, if the detector array is large enough to cover a substantial part of the cardiac volume per rotation. In retrospective ECG-gated acquisitions, multisegment reconstructions require a smaller pitch for similar heart rates compared to monosegment reconstructions to provide sufficient data redundancy with regard to the actual HR.[3, 35] Disadvantages of multisegment reconstructions include the requirement that all segments' imaging should be done within exactly the same phase of the cardiac cycle, and spatially adjacent segments have to be imaged in the same cardiac phase to build-up smooth half-scan intervals. Unfortunately, variations in consecutive cardiac cycles tend to increasingly lower image quality using multisegment reconstruction as compared to monosegment. Moreover, in retrospective gated acquisitions there is a complex relationship between the cardiac cycle duration (heart rate), the rotation speed and multisegment reconstruction.[36, 37]

Other recently introduced *motion-reducing software algorithms* include automated boundary detection and algorithms using information from adjacent cardiac phases within a single cardiac cycle to characterize vessel motion (Figure 8). As such, actual vessel position is determined at the target phase and adaptively compensated to reduce unexpected motion.[38]

Strategies to tackle *arrhythmia* depend on the type of acquisition: (i) for retrospective spiral acquisitions, arrhythmia-induced artifacts can be countered with retrospectively editing of the reconstruction phases based on the continuous ECG registration during the acquisition; (ii) for

prospective and high-pitch spiral scans, the acquisition is automatically suspended and delayed to a following heartbeat when HR changes are detected.[37]

The in-plane *spatial resolution* of CT theoretically approximates the 0.1 and 0.2 mm spatial resolution of intravascular ultrasound and catheter angiography respectively. However, in clinical practice, the in-plane spatial resolution is limited to approximately 0.5 mm by the use of smoothing convolution reconstruction algorithms. Although such a spatial resolution is sufficient for the assessment of significant coronary artery stenosis in vessels of 1.5 mm or more in diameter, it may remain inadequate to assess stent patency and to confidently grade coronary stenosis in severely calcified arteries.[39, 40]

In order to achieve a spatial resolution comparable to catheter angiography, theoretically a 16-fold increase of the radiation dose would be needed since an increase of spatial resolution proportionally increases image noise in standard filtered back projection (FBP) reconstructions.[13] Recently implemented noise-reduction reconstruction algorithms, the so-called iterative reconstruction, in combination with dedicated sharp reconstruction algorithms theoretically allows decoupling of spatial resolution and image noise for better image quality and improved diagnostic performance for the evaluation of in-stent lumen (Figure 9) and coronary calcifications by reducing partial volume effects.[41, 42]

6. Radiation exposure saving and tradeoffs

Initially, coronary CTA was typically associated with radiation doses amongst the highest in medical imaging, with reported effective doses ranging up to 16-32 mSv.[43] Today, radiation exposure has been drastically reduced by technical advances and the implementation of dose efficient strategie while maintaining high quality images.[44] Standard dose reduction strategies are:

(i) dynamic tube current modulation by cardiac phase and tissue density, (ii) tube voltage reduction, and (iii) dynamic collimation in helical acquisition. One study reported a dose reduction of 68% by shifting from retrospective to prospective ECG modulation in patients with a low and stable HR (mean 56 bpm) and a 53% dose reduction by switching the tube voltage from 120 kV to 100 kV.[45, 46] The limitations of tube voltage reduction are increased image noise levels and tube heating. It should therefore be primarily considered in non-obese patients (BMI < 30 kg/m²). Dynamic collimation helps to reduce undesired exposure due to z-axis overbeaming, which is particularly prominent with helical scanning (24% dose saving).[47] More recent strategies to reduce dose are the above-discussed high pitch DSCT acquisition, wide coverage scanners and iterative reconstruction. Compared to standard FBP, hybrid iterative reconstruction refers to an algorithm using mathematical and statistical modeling to reduce image noise while trying to preserve high resolution images by performing repeated backward "iterative" reconstruction cycles, resulting in a reduction of exposure without increase of noise.[42, 48] Although all manufacturers now employ at least one hybrid iterative reconstruction algorithm technology, the implementation and performance of these systems can vary significantly.[42, 49] Further newer systems using full-iterative reconstruction are progressively been implemented. Obviously, largest dose reductions can be achieved by a combination of previously described strategies.[12, 34]

Despite the fact that nowadays the effective dose in Coronary CTA can approach the level of annual background radiation under certain conditions, the female breast tissue dose remains a concern and is reported 10-30 times higher[50] compared to the achievable dose of 2.0 mGy in standard mammography for standard breast thickness.[51]

Besides implementing the earlier described dose efficient scan modes, further breast dose reduction can be achieved by selective in-plane bismuth shielding. Although controversy still exists regarding

its use due to the deleterious impact on image noise, studies do report 40-50% breast dose savings .[52] Moreover, a recent study reported a degradation of the image quality and no effect on the amount of DNA damage using breast shielding during coronary CTA in women.[53]

7. Image quality and future directions

Further improvements in scanner's hardware, software and image processing are promising for better image quality and/or less radiation dose (Figure 9).

Coronary motion will be further reduced by intelligent motion correction algorithms, faster transfer systems and multisource scanning[38, 54], which implementation, alone or in combination is currently limited by the computational demand in image reconstruction power.

Conversely, advances in spectral imaging have paved the way towards photon-counting, a technology in which the whole photonic spectrum is analyzed.[55] However, it is currently not clinically implemented as the limited count rate, energy integrating detection, increased detector pixel crosstalk and electronic noise are major limitations of this technology.[56] Eventually, photon-counting is expected to improve soft-tissue discrimination, to reduce the radiation dose and to provide higher spatial resolution.[57] Compared to dual-energy, photon-counting coronary CTA will provide more detailed information about myocardial and coronary plaque components by analyzing differences in contrast agent concentration and/or spectral attenuation.

In addition, improvement of spatial resolution is expected from ongoing development of detector technology, which could provide a reduction of the slice collimation without significant increase of the radiation exposure. This can currently only be achieved at the cost of increasing noise.[58]

In contrast to hybrid iterative reconstruction algorithms, full-iterative algorithms introduce model-

based forward projection reconstruction analyses, resulting in a further decoupling between the image noise and radiation dose, especially in the low-dose ranges (CTDIvol 2-4 mGy). More than 50% noise suppression is reported compared to the standard filtered back projection. Disadvantages of full-iterative reconstruction algorithms are the computational demands, resulting in substantially longer image reconstruction time.[59 60-63]

8. Conclusion

The recent vendor specific advances have resulted into dramatic improvement of scanning coverage, spatial, temporal and contrast resolution. Easier acquisition, post-processing and better diagnostic confidence are expected from the ongoing image quality improvement. In parallel, patient safety has been improved by dose-reduction strategies and recent achievements indicate that even further dose reductions are to be expected in the near future. There are similarities, but also marked differences between main CT constructors' technologies. It is therefore questionable how far a combination of the main strengths from each constructor into one single "perfect" scanner would not represent a huge step. Meanwhile, the current state-of-the art scanners have already shifted the perception of Coronary CTA being a harmful technique towards a dose-efficient technique that is associated with only minor radiation exposure, paving the way for newer indications such as coronary and cardiac tissue composition imaging.

References

1. Raff GL. Interpreting the evidence: how accurate is coronary computed tomography angiography? J Cardiovasc Comput Tomogr. 2007;1:73-7.
2. Kroft LJ, de Roos A, Geleijns J. Artifacts in ECG-synchronized MDCT coronary angiography. AJR Am J Roentgenol. 2007;189:581-91.
3. Mahesh M, Cody DD. Physics of cardiac imaging with multiple-row detector CT. Radiographics. 2007;27:1495-509.
4. Ghekiere O, Nchimi A, Djekic J, El Hachemi M, Mancini I, Hansen D, et al. Coronary Computed Tomography Angiography: Patient-related factors determining image quality using a second-generation 320-slice CT scanner. Int J Cardiol. 2016;221:970-6.
5. Toth T. Radiation Dose from Multidetector CT. 2 ed: Springer-Verlag Berlin Heidelberg, 2012.
6. Tatsugami F, Higaki T, Nakamura Y, Yamagami T, Date S, Fujioka C, et al. A new technique for noise reduction at coronary CT angiography with multi-phase data-averaging and non-rigid image registration. Eur Radiol. 2015;25:41-8.
7. Leschka S, Stolzmann P, Schmid FT, Scheffel H, Stinn B, Marincek B, et al. Low kilovoltage cardiac dual-source CT: attenuation, noise, and radiation dose. Eur Radiol. 2008;18:1809-17.
8. Tatsugami F, Matsuki M, Nakai G, Inada Y, Kanazawa S, Takeda Y, et al. The effect of adaptive iterative dose reduction on image quality in 320-detector row CT coronary angiography. Br J Radiol. 2012;85:e378-82.
9. Achenbach S, Paul JF, Laurent F, Becker HC, Rengo M, Caudron J, et al. Comparative assessment of image quality for coronary CT angiography with iobitridol and two contrast agents with higher iodine concentrations: iopromide and iomeprol. A multicentre randomized double-blind trial. Eur Radiol. 2016;10.1007/s00330-016-4437-9.
10. Kim EY, Yeh DW, Choe YH, Lee WJ, Lim HK. Image quality and attenuation values of multidetector CT coronary angiography using high iodine-concentration contrast material: a comparison of the use of iopromide 370 and iomeprol 400. Acta Radiol. 2010;51:982-9.
11. Odedra D, Blobel J, Alhumayyd S, Durand M, Jimenez-Juan L, Paul N. Image noise-based dose adaptation in dynamic volume CT of the heart: dose and image quality optimisation in comparison with BMI-based dose adaptation. Eur Radiol. 2014;24:86-94.
12. Chen MY, Shanbhag SM, Arai AE. Submillisievert median radiation dose for coronary angiography with a second-generation 320-detector row CT scanner in 107 consecutive patients. Radiology. 2013;267:76-85.
13. Flohr TG, Raupach R, Bruder H. Cardiac CT: how much can temporal resolution, spatial resolution, and volume coverage be improved? J Cardiovasc Comput Tomogr. 2009;3:143-52.
14. Geleijns J. Physics Background and Radiation Exposure. In: Dewey M, editor. Cardiac CT. Second Edition ed. Heidelberg, Germany 2013. p. 57-70.
15. Huda W, Tipnis S, Sterzik A, Schoepf UJ. Computing effective dose in cardiac CT. Phys Med Biol. 2010;55:3675-84.
16. Deak P, van Straten M, Shrimpton PC, Zankl M, Kalender WA. Validation of a Monte Carlo tool for patient-specific dose simulations in multi-slice computed tomography. Eur Radiol. 2008;18:759-72.
17. Martin CJ. Effective dose: how should it be applied to medical exposures? Br J Radiol. 2007;80:639-47.
18. Maintz D, Seifarth H, Raupach R, Flohr T, Rink M, Sommer T, et al. 64-slice multidetector coronary CT angiography: in vitro evaluation of 68 different stents. Eur Radiol. 2006;16:818-26.
19. Maintz D, Burg MC, Seifarth H, Bunck AC, Ozgun M, Fischbach R, et al. Update on multidetector coronary CT angiography of coronary stents: in vitro evaluation of 29 different stent types with dual-source CT. Eur Radiol. 2009;19:42-9.
20. Bae KT. Intravenous contrast medium administration and scan timing at CT: considerations and approaches. Radiology. 2010;256:32-61.

21. Leiner T, Abbara S. Contrast injection protocols: it is time to get creative! J Cardiovasc Comput Tomogr. 2015;9:28-30.
22. Blankstein R, Bolen MA, Pale R, Murphy MK, Shah AB, Bezerra HG, et al. Use of 100 kV versus 120 kV in cardiac dual source computed tomography: effect on radiation dose and image quality. Int J Cardiovasc Imaging. 2011;27:579-86.
23. Gill MK, Vijayananthan A, Kumar G, Jayarani K, Ng KH, Sun Z. Use of 100 kV versus 120 kV in computed tomography pulmonary angiography in the detection of pulmonary embolism: effect on radiation dose and image quality. Quantitative imaging in medicine and surgery. 2015;5:524-33.
24. Ippolito D, Talei Franzesi C, Fior D, Bonaffini PA, Minutolo O, Sironi S. Low kV settings CT angiography (CTA) with low dose contrast medium volume protocol in the assessment of thoracic and abdominal aorta disease: a feasibility study. Br J Radiol. 2015;88:20140140.
25. Oda S, Utsunomiya D, Yuki H, Kai N, Hatemura M, Funama Y, et al. Low contrast and radiation dose coronary CT angiography using a 320-row system and a refined contrast injection and timing method. J Cardiovasc Comput Tomogr. 2015;9:19-27.
26. Vavere AL, Arbab-Zadeh A, Rochitte CE, Dewey M, Niinuma H, Gottlieb I, et al. Coronary artery stenoses: accuracy of 64-detector row CT angiography in segments with mild, moderate, or severe calcification--a subanalysis of the CORE-64 trial. Radiology. 2011;261:100-8.
27. Abdulla J, Pedersen KS, Budoff M, Kofoed KF. Influence of coronary calcification on the diagnostic accuracy of 64-slice computed tomography coronary angiography: a systematic review and meta-analysis. Int J Cardiovasc Imaging. 2012;28:943-53.
28. den Dekker MA, de Smet K, de Bock GH, Tio RA, Oudkerk M, Vliegenthart R. Diagnostic performance of coronary CT angiography for stenosis detection according to calcium score: systematic review and meta-analysis. Eur Radiol. 2012;22:2688-98.
29. Shapiro MD, Pena AJ, Nichols JH, Worrell S, Bamberg F, Dannemann N, et al. Efficacy of pre-scan beta-blockade and impact of heart rate on image quality in patients undergoing coronary multidetector computed tomography angiography. Eur J Radiol. 2008;66:37-41.
30. Celik O, Atasoy MM, Erturk M, Yalcin AA, Aksu HU, Diker M, et al. Comparison of different strategies of ivabradine premedication for heart rate reduction before coronary computed tomography angiography. J Cardiovasc Comput Tomogr. 2014;8:77-82.
31. Takx RA, Sucha D, Park J, Leiner T, Hoffmann U. Sublingual Nitroglycerin Administration in Coronary Computed Tomography Angiography: a Systematic Review. Eur Radiol. 2015;10.1007/s00330-015-3791-3.
32. Muenzel D, Noel PB, Dorn F, Dobritz M, Rummeny EJ, Huber A. Step and shoot coronary CT angiography using 256-slice CT: effect of heart rate and heart rate variability on image quality. Eur Radiol. 2011;21:2277-84.
33. Johnson TR. Dual-energy CT: general principles. AJR Am J Roentgenol. 2012;199:S3-8.
34. Schuhbaeck A, Achenbach S, Layritz C, Eisentopf J, Hecker F, Pflederer T, et al. Image quality of ultra-low radiation exposure coronary CT angiography with an effective dose <0.1 mSv using high-pitch spiral acquisition and raw data-based iterative reconstruction. Eur Radiol. 2013;23:597-606.
35. Tomizawa N, Komatsu S, Akahane M, Torigoe R, Kiryu S, Ohtomo K. Relationship between beat to beat coronary artery motion and image quality in prospectively ECG-gated two heart beat 320-detector row coronary CT angiography. Int J Cardiovasc Imaging. 2012;28:139-46.
36. Hein PA, May J, Rogalla P, Butler C, Hamm B, Lembcke A. Feasibility of contrast material volume reduction in coronary artery imaging using 320-slice volume CT. Eur Radiol. 2010;20:1337-43.
37. Lesser JR, Flygenring BJ, Knickelbine T, Longe T, Schwartz RS. Practical approaches to overcoming artifacts in coronary CT angiography. J Cardiovasc Comput Tomogr. 2009;3:4-15.
38. Leipsic J, Labounty TM, Hague CJ, Mancini GB, O'Brien JM, Wood DA, et al. Effect of a novel vendor-specific motion-correction algorithm on image quality and diagnostic accuracy in persons undergoing coronary CT angiography without rate-control medications. J Cardiovasc Comput Tomogr. 2012;6:164-71.

39. Hou Y, Ma Y, Fan W, Wang Y, Yu M, Vembar M, et al. Diagnostic accuracy of low-dose 256-slice multi-detector coronary CT angiography using iterative reconstruction in patients with suspected coronary artery disease. Eur Radiol. 2014;24:3-11.
40. Gebhard C, Fiechter M, Fuchs TA, Stehli J, Muller E, Stahli BE, et al. Coronary artery stents: influence of adaptive statistical iterative reconstruction on image quality using 64-HDCT. Eur Heart J Cardiovasc Imaging. 2013;14:969-77.
41. Ebersberger U, Tricarico F, Schoepf UJ, Blanke P, Spears JR, Rowe GW, et al. CT evaluation of coronary artery stents with iterative image reconstruction: improvements in image quality and potential for radiation dose reduction. Eur Radiol. 2013;23:125-32.
42. Willemink MJ, de Jong PA, Leiner T, de Heer LM, Nievelstein RA, Budde RP, et al. Iterative reconstruction techniques for computed tomography Part 1: technical principles. Eur Radiol. 2013;23:1623-31.
43. Mettler FA, Jr., Huda W, Yoshizumi TT, Mahesh M. Effective doses in radiology and diagnostic nuclear medicine: a catalog. Radiology. 2008;248:254-63.
44. Cademartiri F, Maffei E, Arcadi T, Catalano O, Midiri M. CT coronary angiography at an ultra-low radiation dose (<0.1 mSv): feasible and viable in times of constraint on healthcare costs. Eur Radiol. 2013;23:607-13.
45. Bischoff B, Hein F, Meyer T, Hadamitzky M, Martinoff S, Schomig A, et al. Impact of a reduced tube voltage on CT angiography and radiation dose: results of the PROTECTION I study. JACC Cardiovasc Imaging. 2009;2:940-6.
46. Bischoff B, Hein F, Meyer T, Krebs M, Hadamitzky M, Martinoff S, et al. Comparison of sequential and helical scanning for radiation dose and image quality: results of the Prospective Multicenter Study on Radiation Dose Estimates of Cardiac CT Angiography (PROTECTION) I Study. AJR Am J Roentgenol. 2010;194:1495-9.
47. Walker MJ OM, Desai MY, Halliburton SS, Flamm SD. New radiation dose saving technologies for 256-slice cardiac computed tomography angiography. Int J Cardiovasc Imaging. 2009;25:189-99.
48. Wang R, Schoepf UJ, Wu R, Reddy RP, Zhang C, Yu W, et al. Image quality and radiation dose of low dose coronary CT angiography in obese patients: sinogram affirmed iterative reconstruction versus filtered back projection. Eur J Radiol. 2012;81:3141-5.
49. Mieville FA, Gudinchet F, Brunelle F, Bochud FO, Verdun FR. Iterative reconstruction methods in two different MDCT scanners: physical metrics and 4-alternative forced-choice detectability experiments--a phantom approach. Phys Med. 2013;29:99-110.
50. Einstein AJ, Elliston CD, Arai AE, Chen MY, Mather R, Pearson GD, et al. Radiation dose from single-heartbeat coronary CT angiography performed with a 320-detector row volume scanner. Radiology. 2010;254:698-706.
51. Perry N. BM, Wolf C., Törnberg S., Holland R., von Karsa L. European guidelines for quality assurance in breast cancer screening and diagnosis. Fourth edition ed. Luxembourg, Luxembourg 2013.
52. Abadi S, Mehrez H, Ursani A, Parker M, Paul N. Direct quantification of breast dose during coronary CT angiography and evaluation of dose reduction strategies. AJR Am J Roentgenol. 2011;196:W152-8.
53. Cheezum MK, Redon CE, Burrell AS, Kaviratne AS, Bindeman J, Maeda D, et al. Effects of Breast Shielding during Heart Imaging on DNA Double-Strand-Break Levels: A Prospective Randomized Controlled Trial. Radiology. 2016;281:62-71.
54. Wang G, Yu H, Ye Y. A scheme for multisource interior tomography. Med Phys. 2009;36:3575-81.
55. de Vries A, Roessl E, Kneepkens E, Thran A, Brendel B, Martens G, et al. Quantitative spectral K-edge imaging in preclinical photon-counting x-ray computed tomography. Invest Radiol. 2015;50:297-304.
56. Yu Z, Leng S, Jorgensen SM, Li Z, Gutjahr R, Chen B, et al. Evaluation of conventional imaging performance in a research whole-body CT system with a photon-counting detector array. Phys Med Biol. 2016;61:1572-95.

57. Boussel L, Coulon P, Thran A, Roessl E, Martens G, Sigovan M, et al. Photon counting spectral CT component analysis of coronary artery atherosclerotic plaque samples. Br J Radiol. 2014;87:20130798.
58. Pelc NJ. Recent and future directions in CT imaging. Ann Biomed Eng. 2014;42:260-8.
59. Nishiyama Y, Tada K, Mori H, Maruyama M, Katsube T, Yamamoto N, et al. Effect of the forward-projected model-based iterative reconstruction solution algorithm on image quality and radiation dose in pediatric cardiac computed tomography. Pediatr Radiol. 2016;10.1007/s00247-016-3676-x.
60. Sucha D, Willemink MJ, de Jong PA, Schilham AM, Leiner T, Symersky P, et al. The impact of a new model-based iterative reconstruction algorithm on prosthetic heart valve related artifacts at reduced radiation dose MDCT. Int J Cardiovasc Imaging. 2014;30:785-93.
61. Stehli J, Fuchs TA, Bull S, Clerc OF, Possner M, Buechel RR, et al. Accuracy of coronary CT angiography using a submillisievert fraction of radiation exposure: comparison with invasive coronary angiography. J Am Coll Cardiol. 2014;64:772-80.
62. Wang W, Ionita C, Huang Y, Qu B, Panse A, Jain A, et al. Region-of-Interest Micro-Angiographic Fluoroscope Detector Used in Aneurysm and Artery Stenosis Diagnoses and Treatment. Proc SPIE Int Soc Opt Eng. 2012;8313.
63. den Harder AM, Willemink MJ, de Jong PA, Schilham AM, Rajiah P, Takx RA, et al. New horizons in cardiac CT. Clin Radiol. 2016;S0009-9260(16)00044-1 [pii] 10.1016/j.crad.2016.01.022.

Table 1: Main coronary CTA artifacts causes and solutions.

Artifacts	Problem	Cause	Solution
Blurring	Motion	- Heart rate > acquisition speed - Respiration during acquisition - Inappropriate cardiac cycle phase reconstruction	- Heart rate control (β- or Calcium channel blockade, ivabradine) - Breath-hold instructions - Optimal cardiac cycle phase reconstruction - Use multisegment acquisition/reconstruction - Intelligent boundary detection
Stairstep or banding	- Motion - Cardiac cycle phase misregistration	- Heart rate variation (tachycardia/arrhythmia) - ECG signal failure - Respiration during acquisition	- Heart rate control (β- or Calcium channel blockade, ivabradine) - Optimal cardiac cycle phase reconstruction - ECG editing - Pre-scan ECG quality check - Breath-hold instructions
Streak	Dark bands through objects adjacent to high-attenuating	- Metallic implants, surgical clips and coronary stents - Vessel filled with high iodine concentration	- Avoid undiluted contrast (use saline bolus flush)

	structures (beam hardening effect)		-Use a high kilovoltage monoenegetic x-ray beam (dual-energy CT)
Blooming	High-attenuating objects appear larger than they are	- Coronary calcifications - Metallic implants, clips and coronary stents	- Use high spatial resolution reconstruction algorithms + iterative reconstruction (to decrease the noise) - Use the smallest available focal spot -Use a high kilovoltage monoenegetic x-ray beam (dual-energy CT)
Windmill	Highly attenuating structures are surrounded by low attenuating rims, and low attenuating structures appear larger and have a “fan-like” appearance	- Moving structures during acquisition - Heart rate > temporal resolution > spiral acquisition pitch	- Prefer sequential acquisition - Heart rate control (β- or Calcium channel blockade, ivabradine) - Optimize spiral scanning pitch
Low-attenuating	Air bubbles	- Air within the contrast material bolus - Surgery	Check intravenous line before contrast injection

Table 2: Top four vendors recent technological advances in coronary CTA

	Vendor			
Item	**General Electric**	**Philips**	**Siemens**	**Toshiba**
Arrhythmia	- Adaptative gating - ECG R-peak Editor	- Auto-arrhythmia detection - ECG R-peak Editor	-Adaptive Cardio Sequence - ECG R-peak Editor	-Arrhythmia detection - ECG R-peak Editor
Gantry rotation speed	280 ms	270 ms	250 ms	275 ms
Maximum z-axis coverage/rotation (sequential)	16 cm	8 cm	7,68 cm	16 cm
Number of X-ray tubes	1	1	1 or 2	1
Current detector technology	Gemstone Clarity	NanoPanel prism (IQon)	Stellar^{Infinity}	^{PURE}Vision
Hybrid noise reduction software acronym	ASIR (Adaptive Statistical Iterative Reconstruction)	iDose4 (i-dose iterative reconstruction)	IRIS (Iterative Reconstructions in Image Space) SAFIRE (Sinogram Affirmed Iterative Reconstruction)	AIDR (Adaptive Iterative Dose Reduction) AIDR 3D (Adaptive Iterative Dose Reduction 3D)

			ADMIRE (Advanced Modeled Iterative reconstruction)	
Full noise reduction software acronym	MBIR or Veo (Model-Based Iterative reconstruction)	IMR (Iterative Model-Based reconstruction)		FIRST (Forward Projected Model-based Iterative Reconstruction SoluTion

Figure legends

Figure 1: Long-axis curvilinear reformation of the right coronary artery on a prospective ECG-triggered Coronary CTA scan shows cardiac motion-related blurring artifact of the second segment (A, circle), due to high HR, as shown on the simultaneously recorded ECG (B, average HR = 75 bpm).

Figure 2: Long-axis curvilinear reformation of the right coronary artery on a retrospective ECG-gated Coronary CTA shows stairstep artifacts (A, arrows) due to cardiac arrhythmia, as shown on the simultaneously recorded ECG (B).

Figure 3: High-attenuating Coronary CTA artifacts on long-axis curvilinear reformation images of the left anterior descending artery: (A) is a 65-year-old male with history of multiple coronary stentings. Two stents are visible, with the proximal one being highly attenuating (arrows) and preventing lumen visualization, while the distal stent exhibits a better luminal visibility (arrowhead). (B) is a 69-year-old male with diabetes mellitus. Extensive calcifications prevent luminal assessment (arrows).

Figure 4: Coronal (A) and axial (B) reformats of Coronary CTA shows low density artifacts (arrows) around the contrast-filled right coronary artery, due to inadequate spiral pitch with regard to HR.

Figure 5: Major changes in Coronary CTA technology over the first decade of the 21th century.

While the number of detectors and the coverage has been increased more than 10-fold, the gantry rotation time has been decreased by more than a half**.**

Figure 6: Step-by-step strategies to optimize image quality and radiation dose with coronary CTA

Different actions can be implemented to produce sizable effects towards image quality and radiation dose optimization with current coronary CTA technology. The gray boxes highlight the role of expected technological advances.

Coronary CTA = coronary computed tomography angiography; HR= heart rate; BMI = body mass index; BP = Blood pressure; kV = Kilovoltage; mA =Milliampere; IR = iterative reconstruction

Figure 7: Coronary CTA in a 41-year-old male with a HR of 92 bpm. Excellent image quality (arrows in A) of the right coronary artery is obtained on the long-axis curvilinear and orthogonal reformations after multi-segment reconstruction of whole-heart data acquired over two cardiac cycles (arrows in B). The reconstruction of a single-segment data (arrow in D), resulted into a lower temporal resolution and caused a poorer image quality (arrows in C).

Figure 8: Long and short axis multiplanar reformats of the right coronary artery on a prospective ECG-triggered acquisition with average HR of 67 bpm without (A and B) and with a temporal resolution improvement algorithm (C and D), allowing minimization of the cardiac motion-related blurring on the right coronary artery and assessment of the stent patency (white arrows in A and C).

Figure 9: Coronary CTA in a 55-year-old male with history of left main trunk, left anterior descending and circumflex artery stenting. Two different reconstructions algorithms (Standard in A and sharper in B) are performed using iterative reconstruction techniques and the smallest field of view (8cm). With the sharper reconstruction algorithm, higher image noise is seen as compared to the standard reconstruction, but more details of the proximal circumflex artery severe in-stent

restenosis are seen (white arrow in B), with a better correlation with catheter coronary angiography (white arrow in C).

Figure 1a

Figure 1b

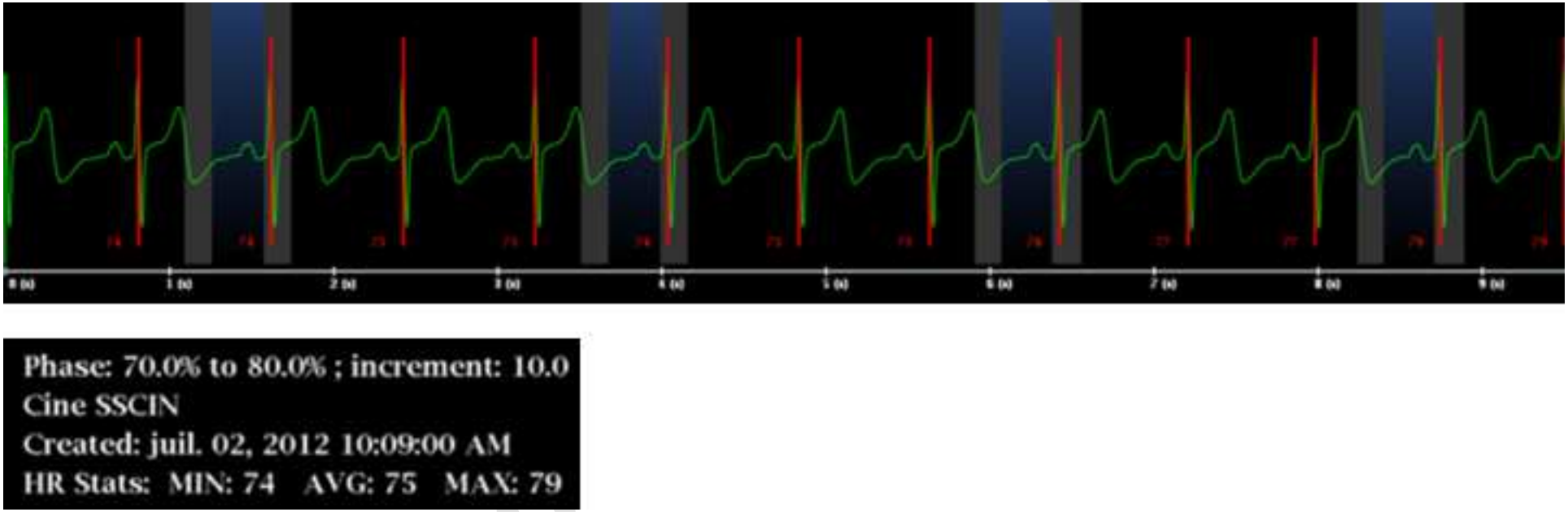

Figure 2a

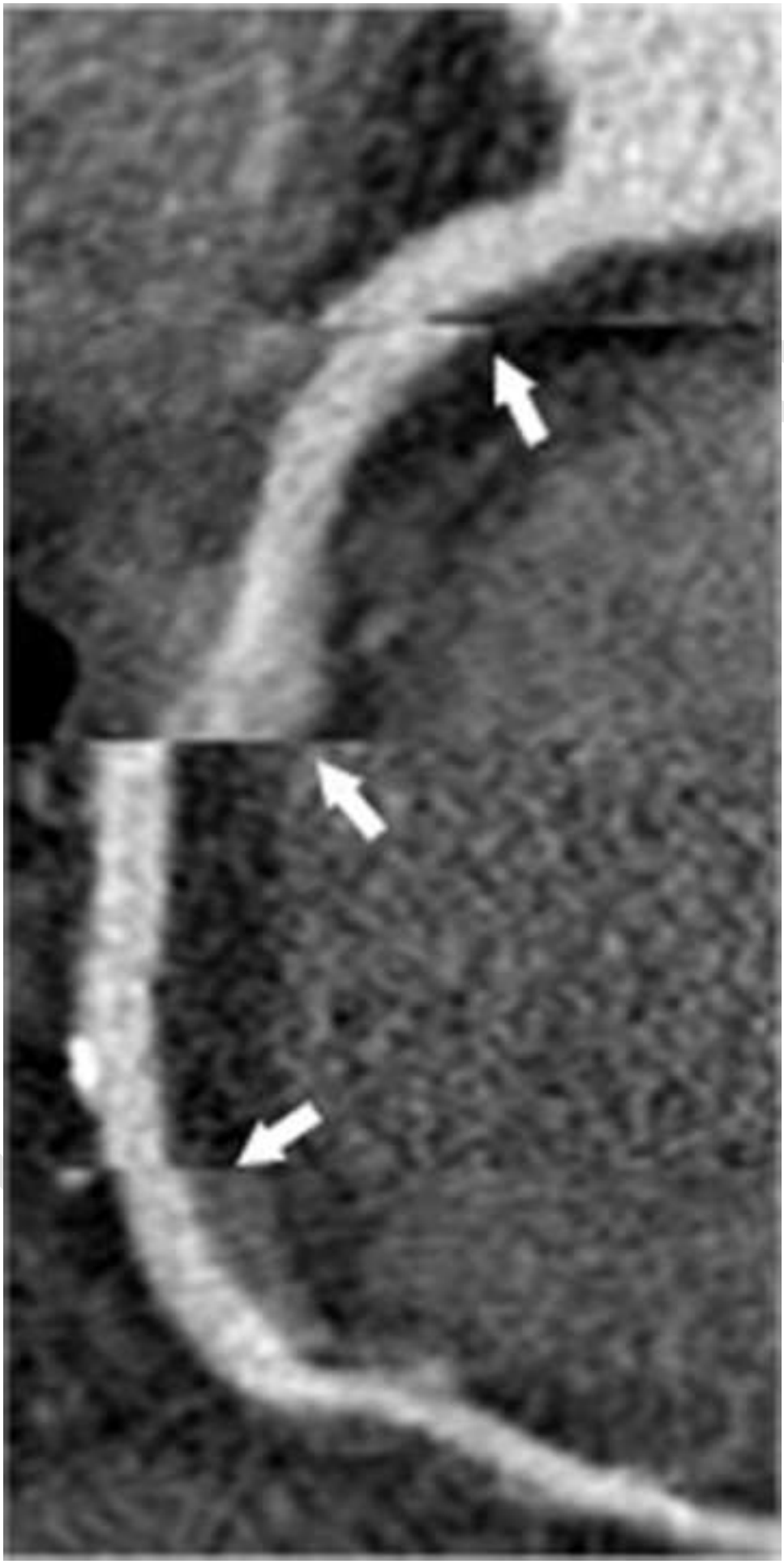

Figure 2b

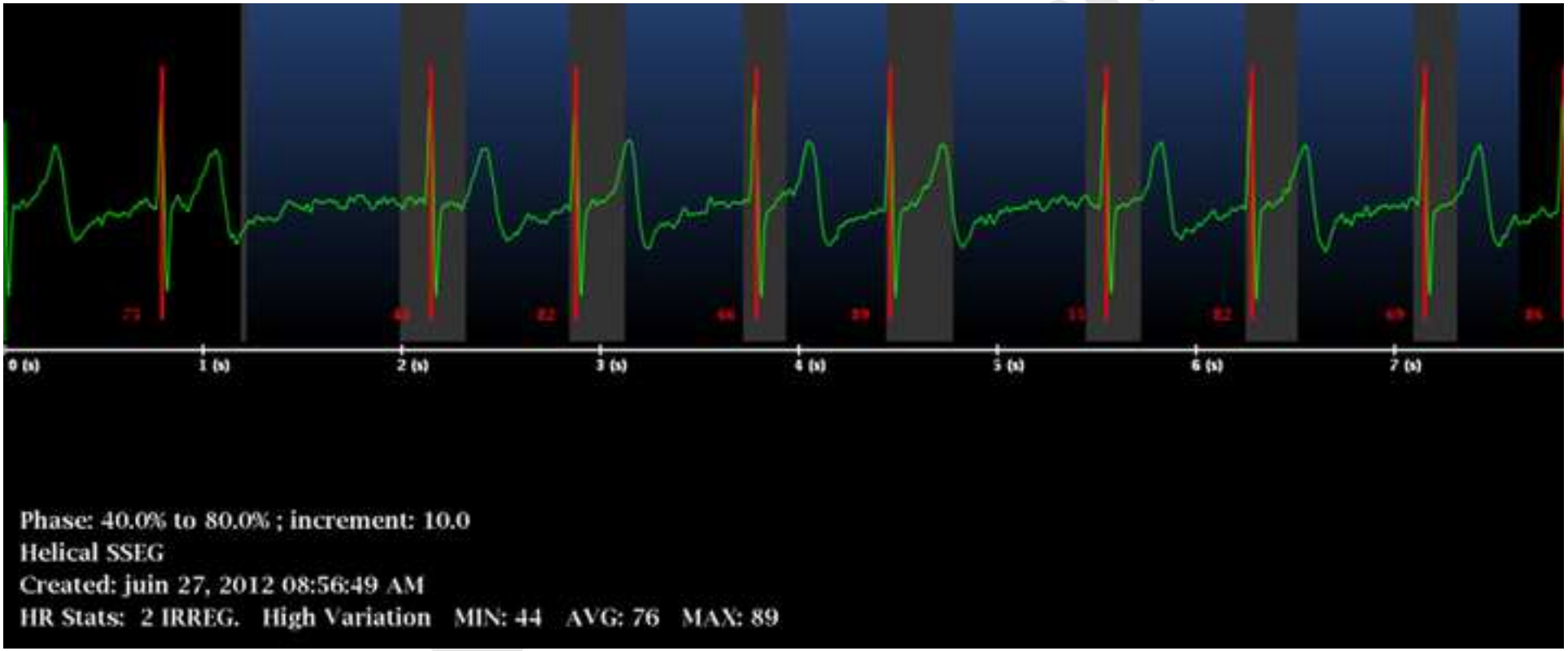

Figure 3a

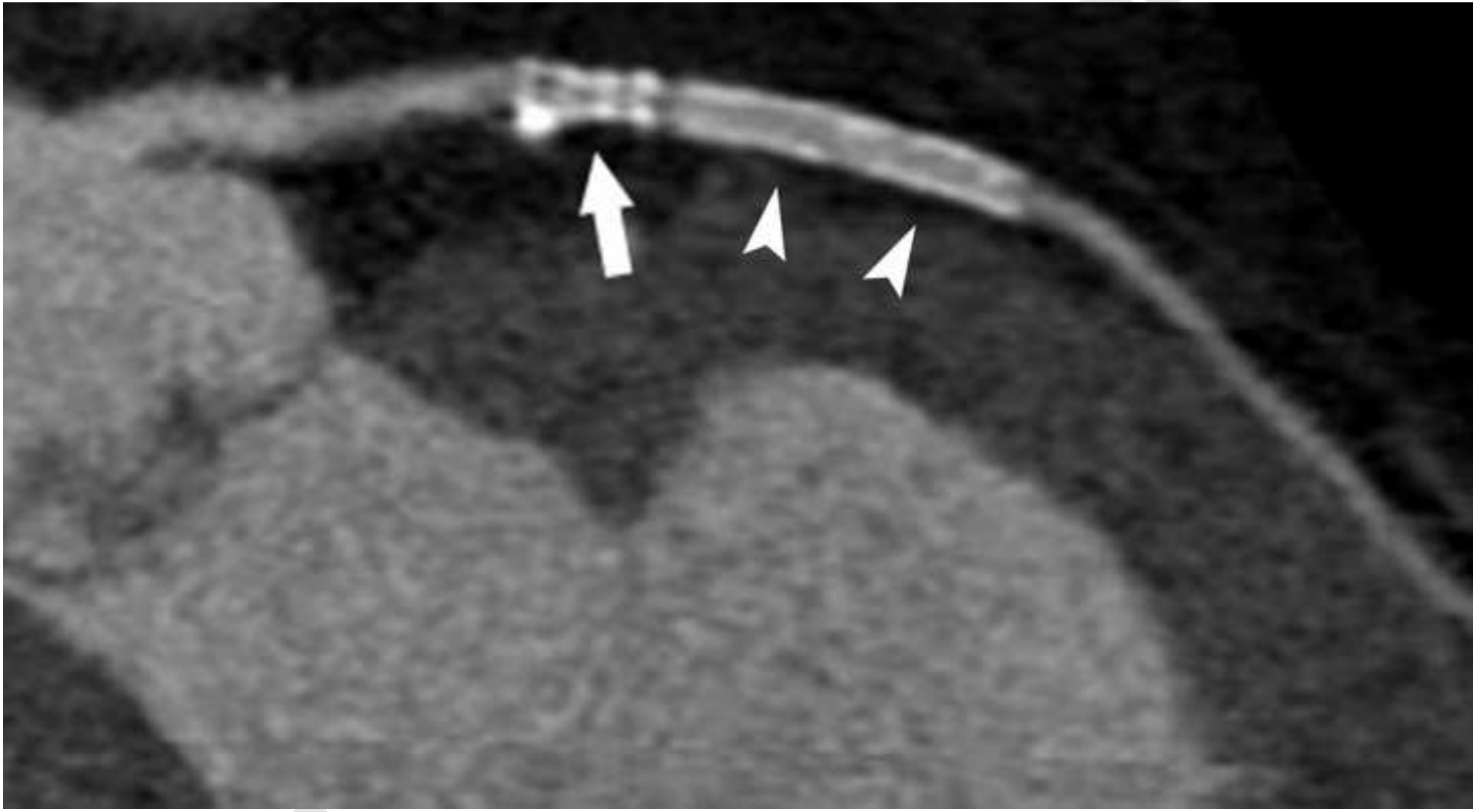

Figure 3b

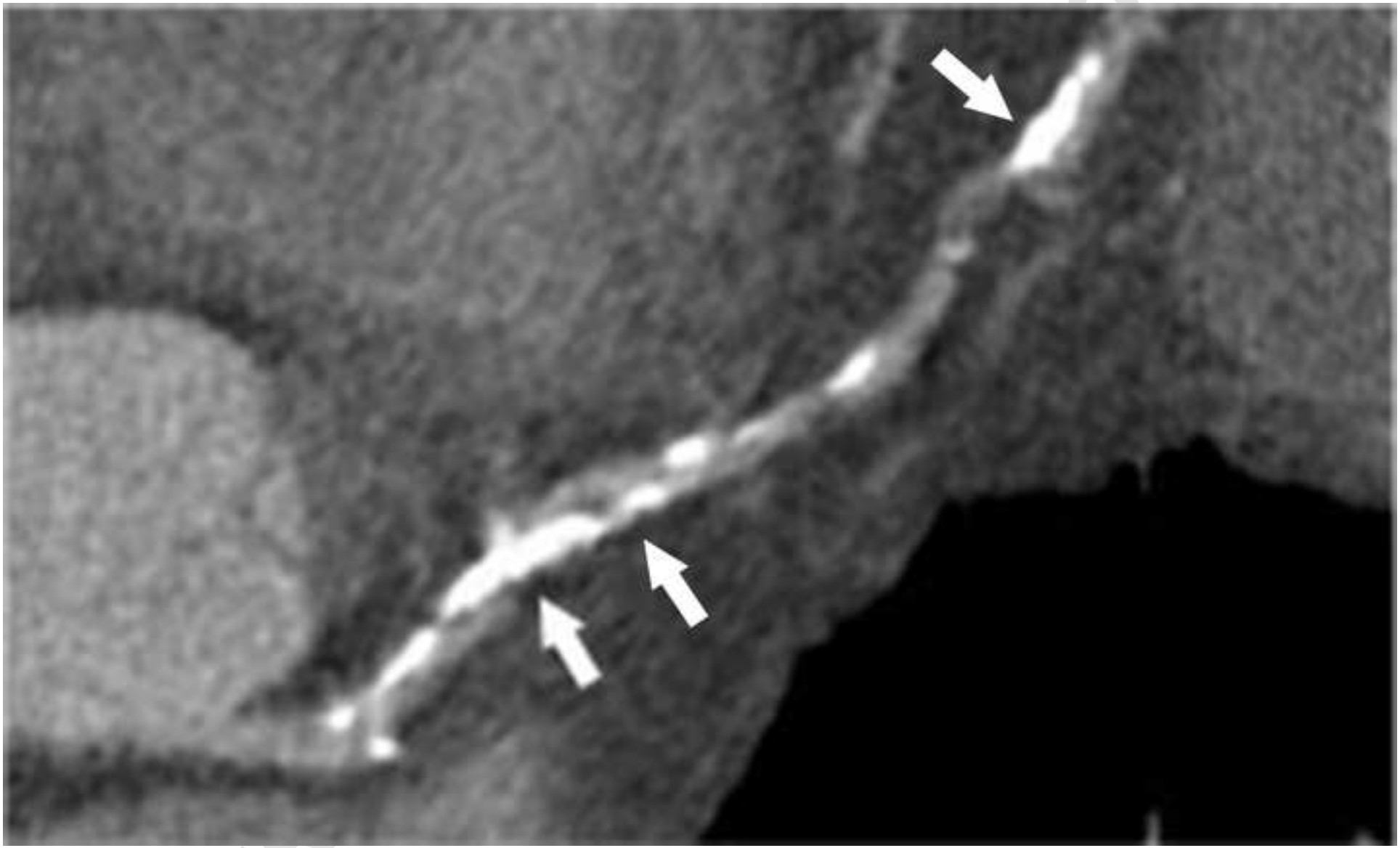

Figure 4a

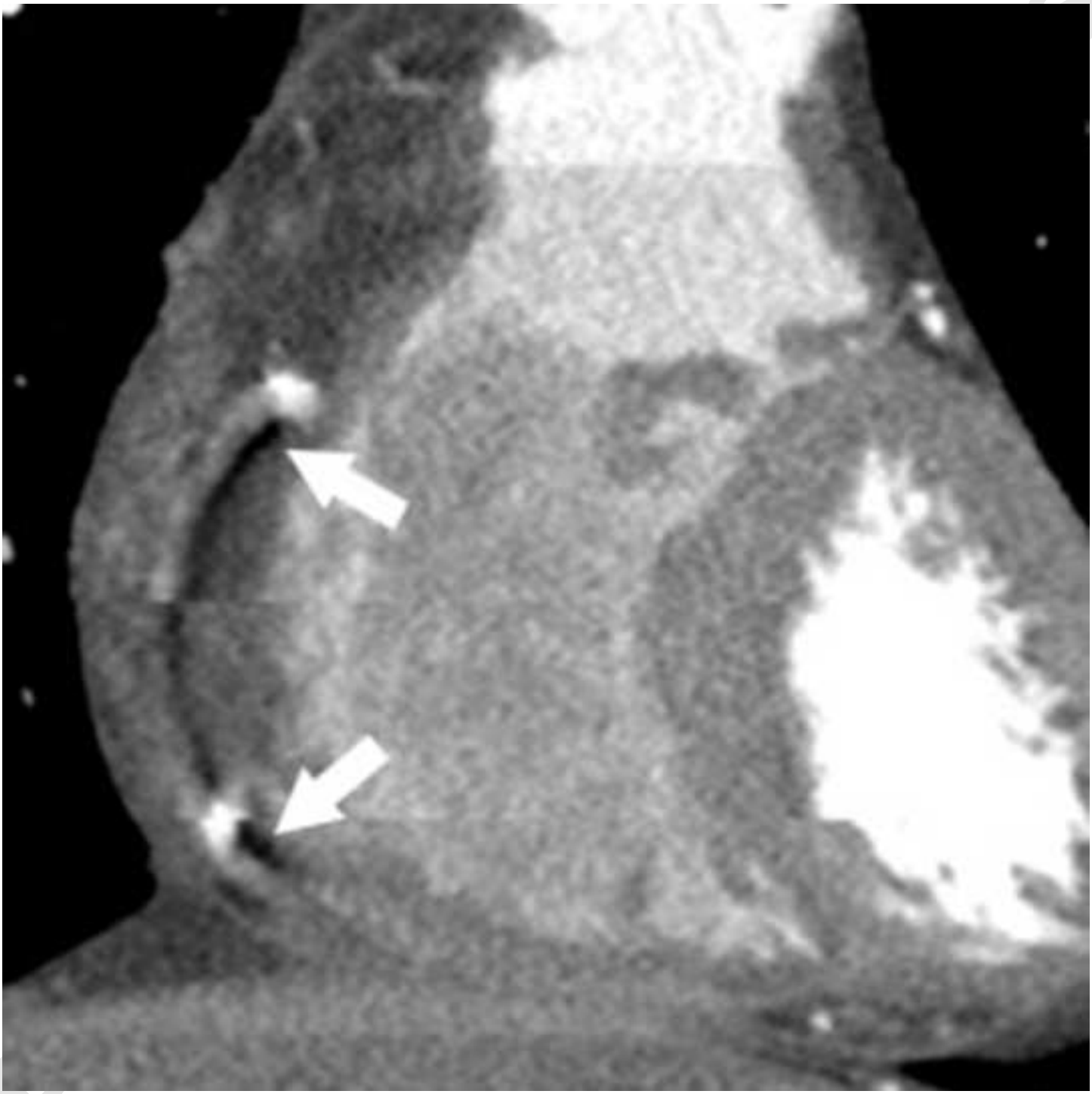

Figure 4b

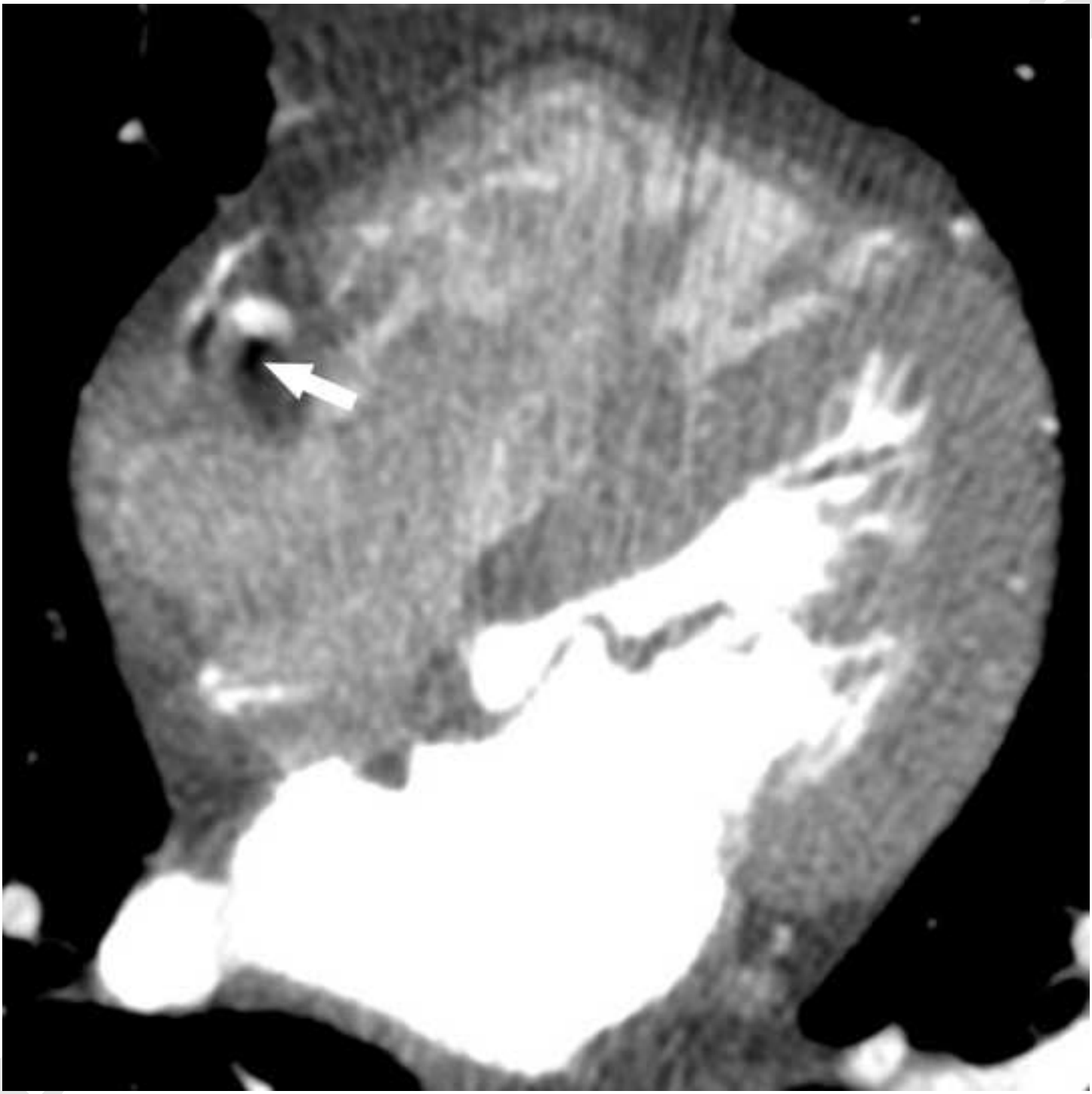

Figure 5

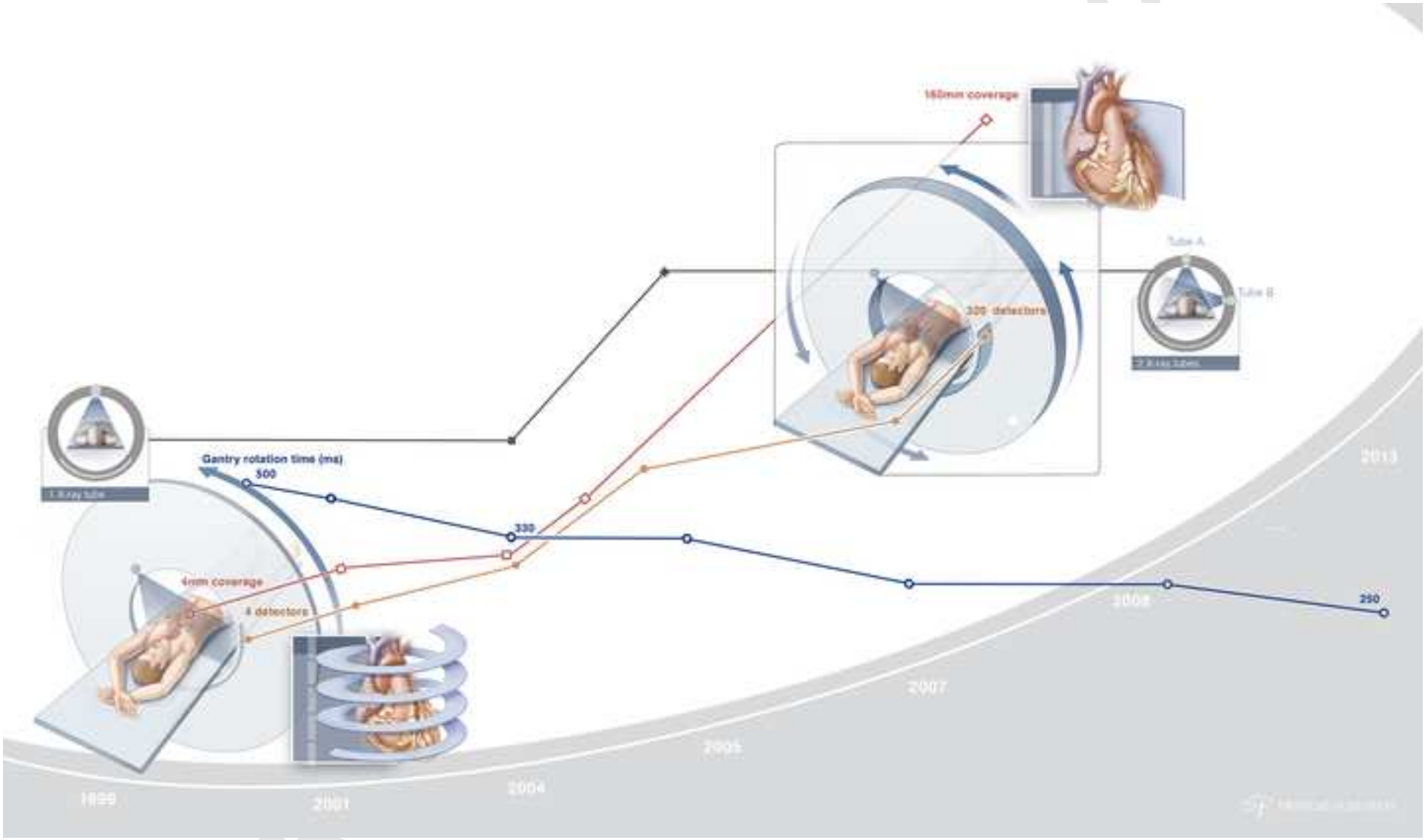

Figure 6

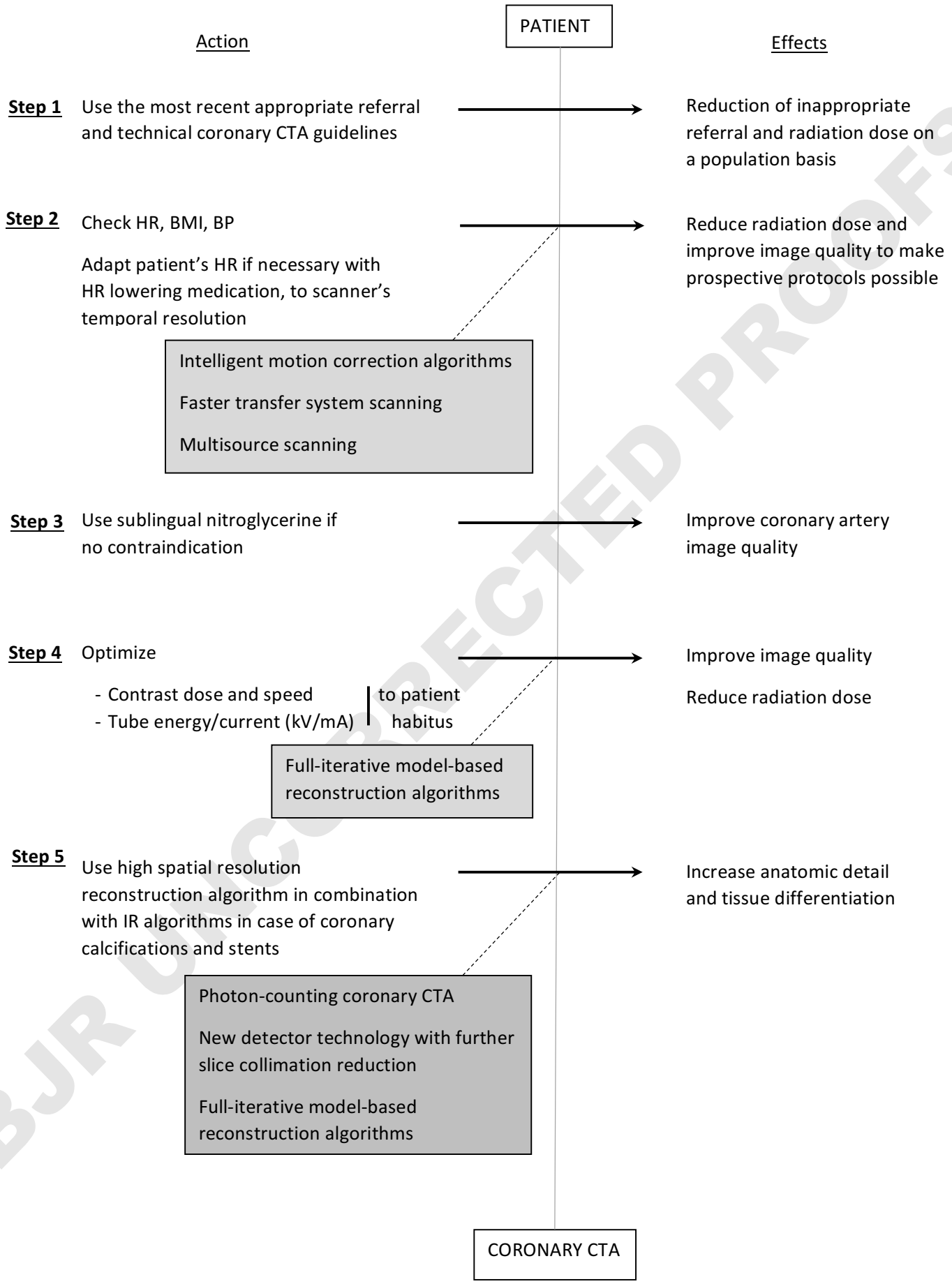

Figure 7a

Click here to download Figure Fig. 7a.tiff

Figure 7b

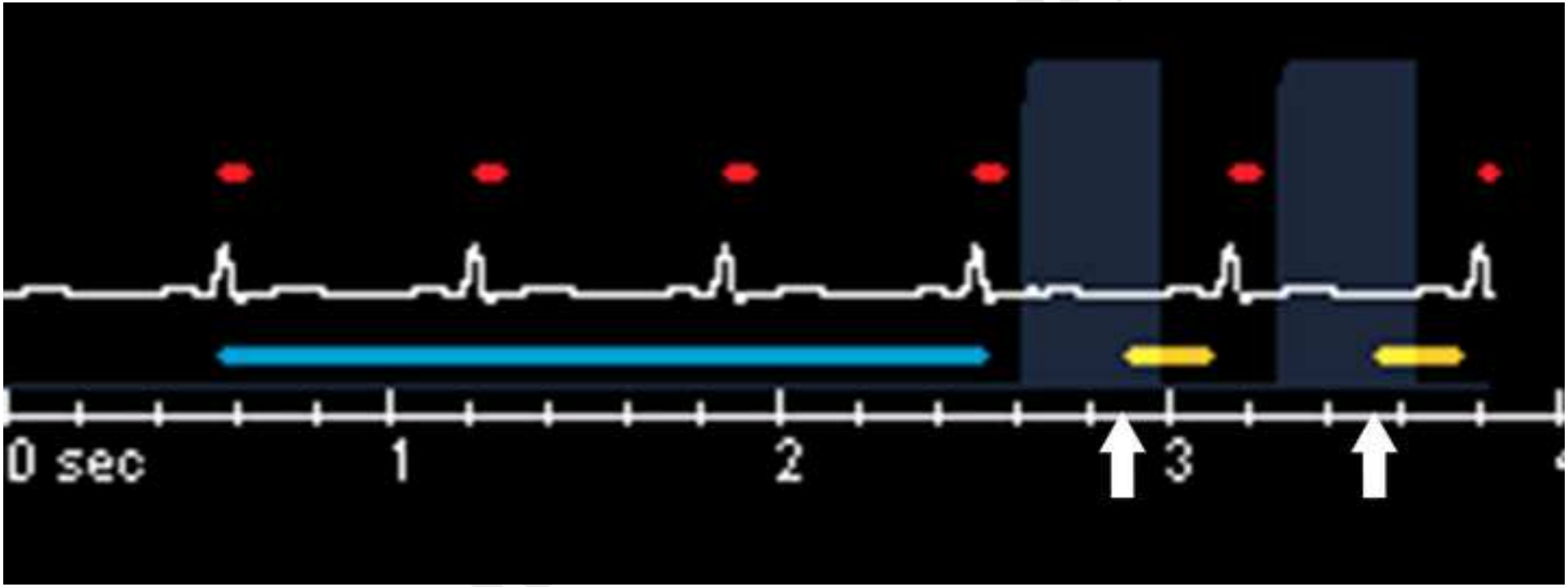

Figure 7c

Click here to download Figure Fig. 7c.tiff

Figure 7d

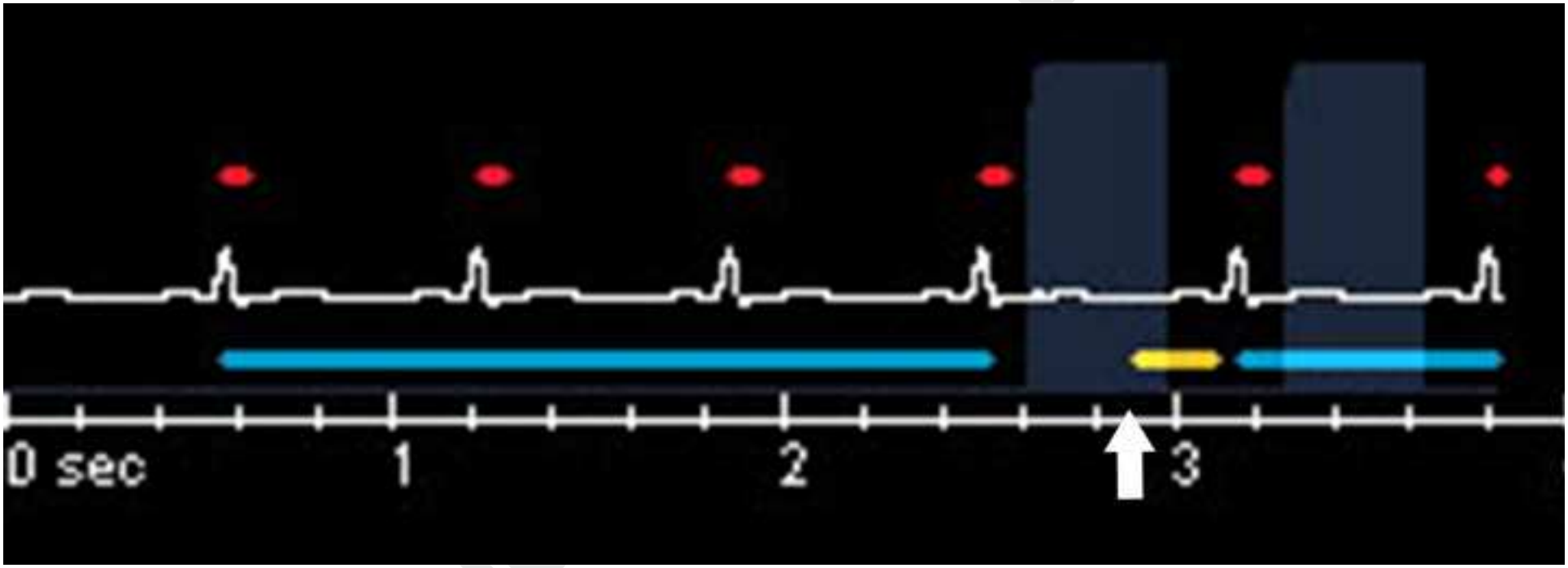

Figure 8a

Figure 8b

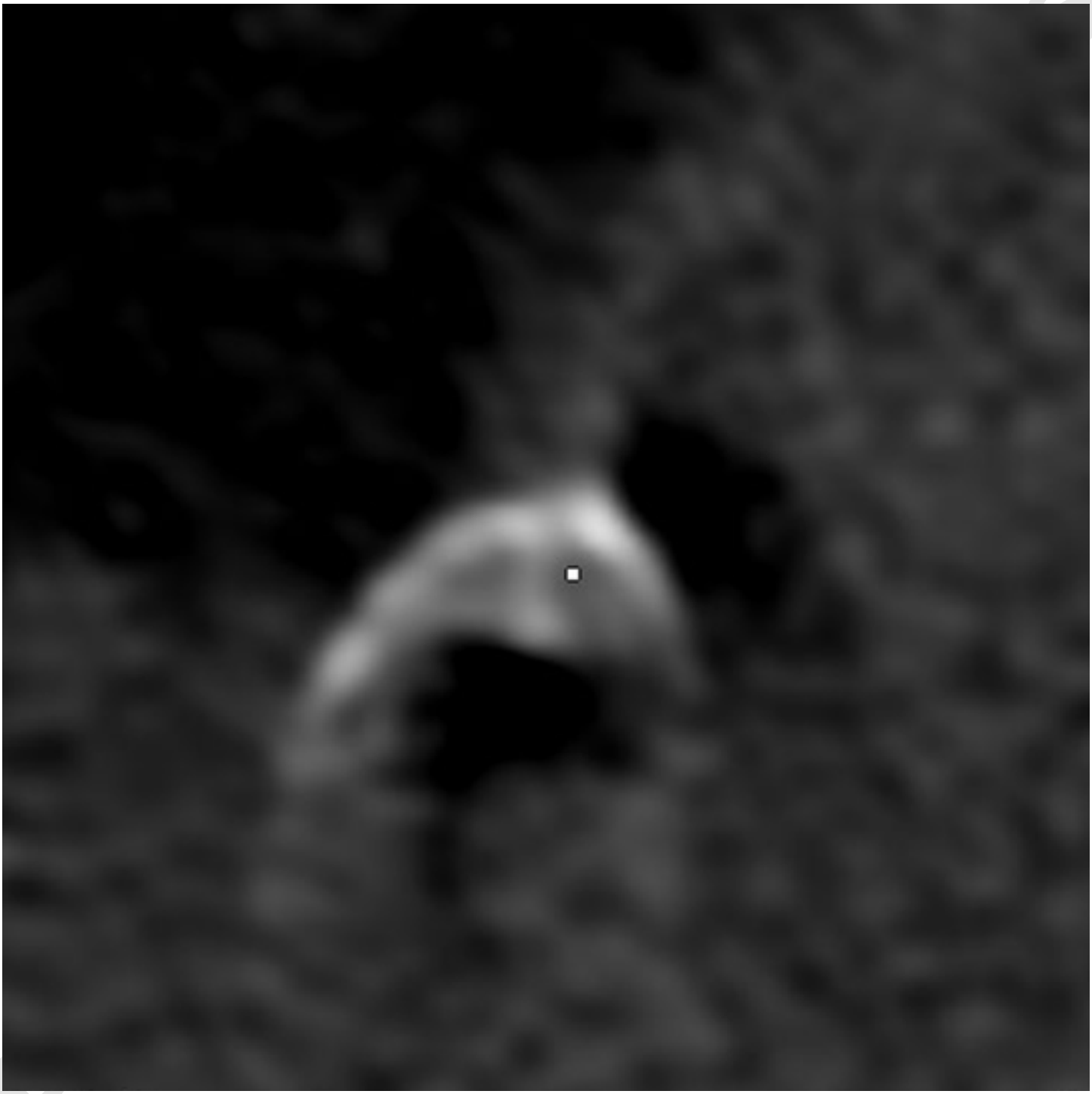

Figure 8c

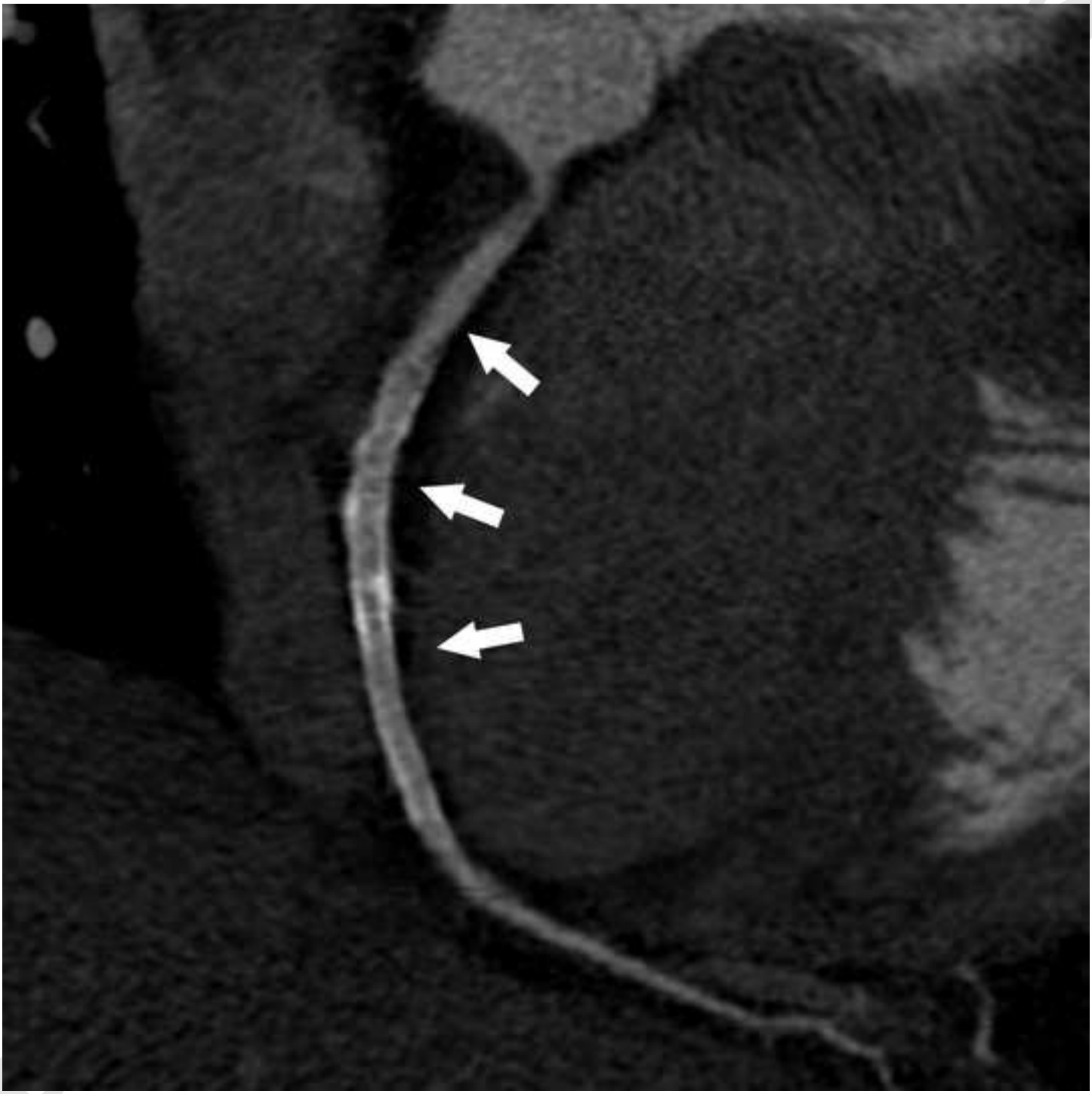

Figure 8d

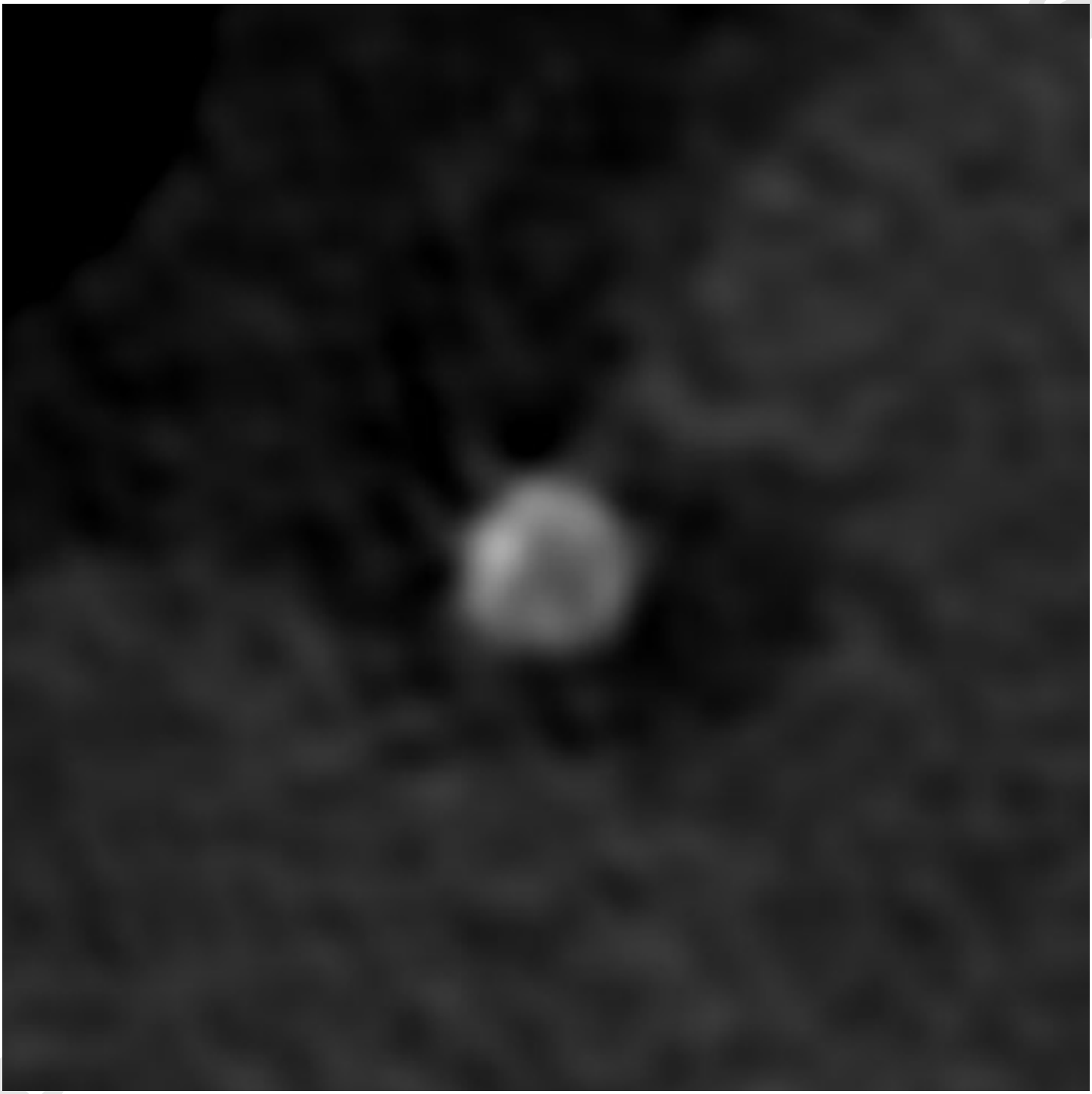

Figure 9a

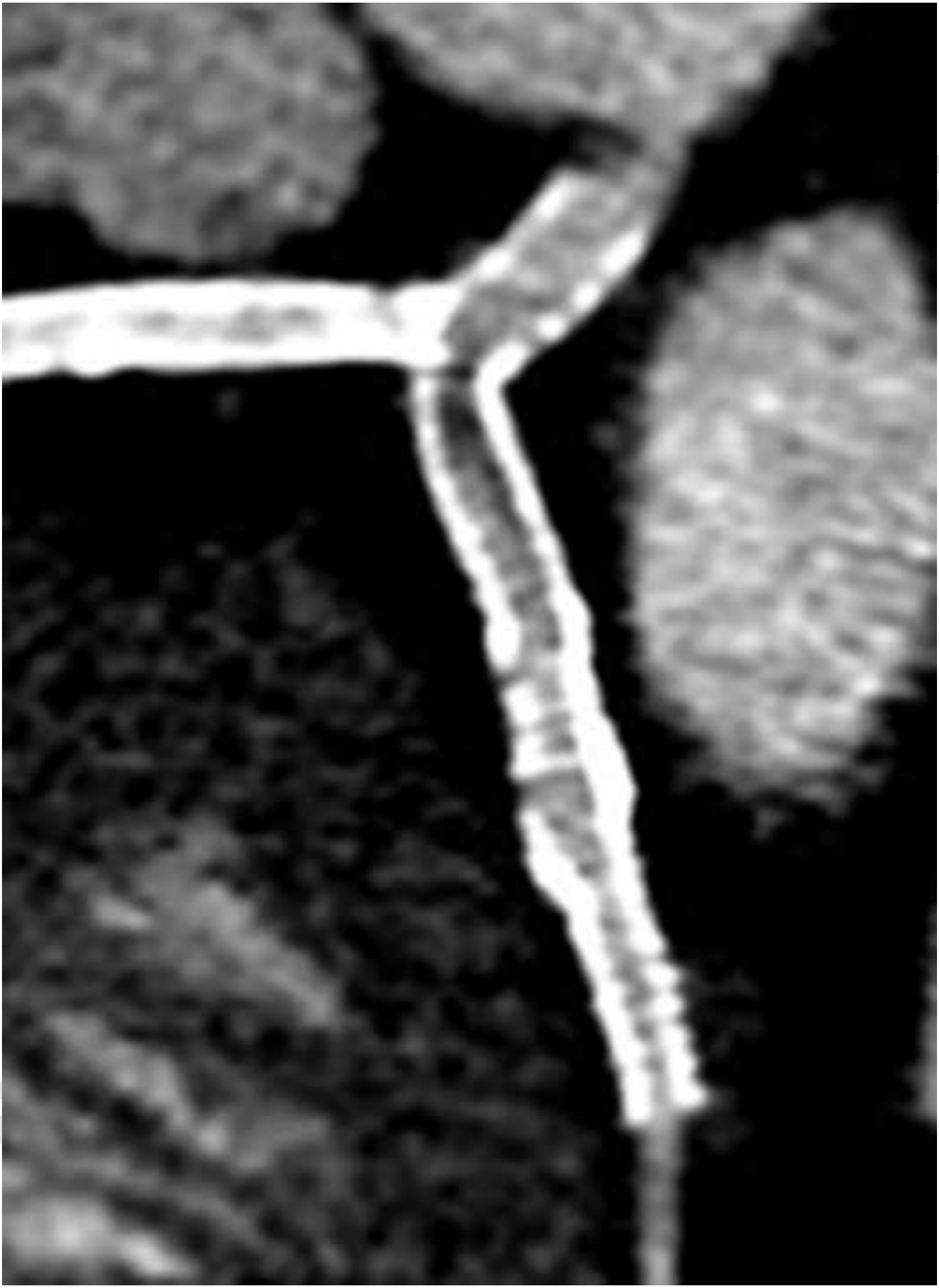

Figure 9b

Click here to download Figure Fig. 9b.tiff

Figure 9c

Click here to download Figure Fig. 9c.tiff